

# Investigation of Thermal Characterization of a Thermally Enhanced FC-PBGA Assembly

C. F. Lin<sup>1</sup>, G. H. Wu<sup>1\*</sup>, S. H. Ju<sup>2</sup>

<sup>1</sup>Department of Mechanical Engineering, National Cheng-Kung University, Tainan, Taiwan

<sup>2</sup>Department of Civil Engineering, National Cheng-Kung University, Tainan, Taiwan

Email: \*d1014519@mail.ncku.edu.tw, juju@mail.ncku.edu.tw

Received January 1, 2013; revised February 1, 2013; accepted February 10, 2013

Copyright © 2013 C. F. Lin *et al.* This is an open access article distributed under the Creative Commons Attribution License, which permits unrestricted use, distribution, and reproduction in any medium, provided the original work is properly cited.

## ABSTRACT

In this paper, three-dimensional finite element analysis using the commercial ANSYS software is performed to study the thermal performance of a thermally enhanced FC-PBGA (flip-chip plastic ball grid array) assembly in both natural and forced convection environments. The thermally enhanced FC-PBGA assembly is a basic FC-PBGA assembly with a lid attached on top, after which an extruded-fin heatsink is attached on the top of the lid. The finite element model is complete enough to include key elements such as bumps, solder balls, substrate, printed circuit board, extruded-fin heatsink, lid, vias, TIM1 (thermal interface material 1), TIM2 (thermal interface material 2), lid-substrate adhesive and ground planes for both signal and power. Temperature fields are simulated and presented for several package configurations. Thermal resistance is calculated to characterize and compare the thermal performance by considering alternative design parameters of the polymer-based materials and the thermal enhancement components. The polymer-based materials include underfill, TIM1, TIM2, lid-substrate adhesive and substrate core material. The specific thermal enhancement components are the extruded-fin heatsink and the lid.

**Keywords:** Polymer-Based Materials; Flip-Chip Packaging; Finite Element Methods

## 1. Introduction

Due to increasing demand for high density, high I/O, high performance electrical application and flip-chip plastic ball grid array (FC-PBGA) packaging are rapidly becoming the package of choice. FC-PBGA technology offers many advantages over the popular PBGA. Commonly stated advantages of FC-PBGA are higher packaging density, shorter leads, lower inductance, better noise control, smaller device footprint and lower package profile [1]. A typical basic FC-PBGA assembly (*i.e.* without thermal enhancement) is shown schematically in **Figure 1**. Heat dissipated from the chip follows two major paths. One path goes from the top of the chip to the ambient environment. The other path goes from the chip to the substrate to the solder balls to the PCB and finally to the ambient.

Due to the rapid increase of power and packaging densities, thermal issues have become critical factors for reliability. Various thermal enhancements have been developed for the basic FC-PBGA package to improve

thermal performance. Gugliermetti and Grignaffini [2] analyzed theoretically the thermal performance of parallel stacks of in-line plate fin heat sinks. They reported that a fin efficiency parameter, like that used for constant cross-section fin in an isothermal fluid flow, can be introduced to express both the local and overall heat transfer balances. Many numerical and experimental studies in recent years have focused on thermal enhancement techniques for FC-PBGA packages. Joiner [3] numerically and experimentally compared the thermal performance between a FC-CBGA with a heatsink and a FC-PBGA with a heatsink. He reported that both FC-PBGA and FC-CBGA packages can be used for relatively high power applications. If a heatsink is implemented, then both package types yield comparable thermal performance. Chen *et al.* [4] proposed a finite element methodology to predict the thermal resistance of both FC-PBGA with a bare die and FC-PBGA with a metal cap. They reported that the material of the metal cap slightly influenced the thermal resistance when the heat dissipation was saturated through the metal cap. Luo *et al.* [5] analyzed by finite element methodology, a whole mobile phone system, by observing the system response to one

\*Corresponding author.

source. They reported that material with thermal conductivity can be added between the chip and the bottom case to enhance the thermal management under natural convection. Menon *et al.* [6] studied the thermal performance of the package on package structure in natural environments using finite element modeling methodology and analyzing the effect of die power on the logic and memory dies.

This present paper considers three-dimensional finite element simulation of a thermally enhanced FC-PBGA assembly in both natural and forced air convection environments, using the commercial software ANSYS [7]. The thermally enhanced FC-PBGA assembly is a basic FC-PBGA assembly with a lid attached on top, after which an extruded-fin heatsink is attached on the top of the lid, as seen in **Figure 2** and denoted in the following as an FC-PBGA/lid/heatsink assembly. The finite element model is complete enough to include key elements such as bumps, solder balls, substrate, printed circuit board, extruded-fin heatsink, lid, vias, TIM1, TIM2, lid-substrate adhesive and ground planes for both signal and power. Temperature fields are simulated and presented for several package configurations. Thermal resistance is calculated to characterize and compare the thermal performance by considering alternative design parameters of the polymer-based materials and the thermal enhancement components. The polymer-based materials include underfill, TIM1, TIM2, lid-substrate adhesive and substrate core material. The specific thermal enhancement components are the extruded-fin heatsink and the lid.

## 2. Finite Element Modeling

### 2.1. Description of FC-PBGA/Lid/Heatsink Assembly

In the following we consider an FC-PBGA/lid/heatsink

assembly, as seen in **Figure 2**. This assembly has a silicon chip size of  $7.4 \times 5.4 \times 0.74$  mm, with 256 solder bumps distributed over the base. The chip is first bonded to an organic substrate with solder bump interconnects. The space between chip and substrate is then filled with epoxy-based underfill material. The purpose of the underfill is to release the thermo-mechanical stress of the solder bumps due to coefficient of thermal expansion mismatch between the silicon chip and the organic substrate. The  $25 \times 25 \times 1.0$  mm substrate contains six buried metal layers and also a 0.05 mm solder mask layer on both the upper and lower surfaces. This FC-PBGA package is mounted on a four-layer (2s2p) PCB with solder balls 0.77 mm in diameter and 0.45mm in height. The solder balls are patterned as a depopulated array in which a  $9 \times 9$  array of central balls is removed from a full array of  $19 \times 19$  solder balls. The  $100 \times 100 \times 1.52$  mm PCB also contains a 0.05 mm solder mask layer on both top and bottom surfaces and is exposed to the air in a horizontal package-up position, as seen in **Figure 2**. The core material of the substrate is FR-5 laminate, while the core material of the PCB is FR-4 laminate. Vias connect various layers within the substrate and the PCB for reasons of electrical and/or thermal conduction and have a much higher thermal conductivity value (300 - 400 W/m·K) than the organic core material (0.2 - 0.4 W/m·K). Heat is conducted by the vias from the chip through the solder balls and into the PCB in the out of plane (Z) direction. The present finite element model assumes that each solder ball or solder bump is associated with a through-via in the substrate and in the PCB. Vias in the substrate are solid copper with a diameter of 0.05 mm. Vias in the PCB are hollow copper with outer and inner diameters of 0.25 and 0.20 mm, respectively.

An aluminum lid is attached on top of the substrate, covering the chip. The contact between any two surfaces

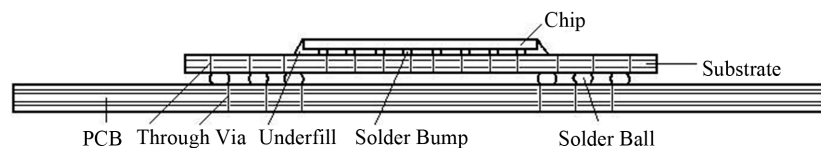


**Figure 1.** A typical basic FC-PBGA assembly.

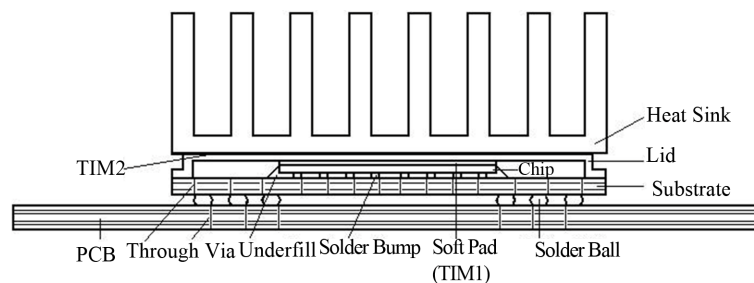


**Figure 2.** Cross section of the FC-PBGA/lid/heatsink assembly.

creates a resistance that may greatly reduce heat conduction efficiency across the contact surface unless a thermal interface material (TIM) is used. A soft pad is applied between the chip and the lid. The soft pad is silicone elastomers filled with high conductivity particles such as boron nitride and has a thermal conductivity of  $3.7 \text{ W/m}\cdot\text{K}$  and denoted in the following as TIM1. The lid has a typical thickness of  $0.5 \text{ mm}$  and is bonded to the substrate with a layer of B-stage epoxy  $0.15 \text{ mm}$  thick. The epoxy resin, denoted in the following as lid-substrate adhesive, contains alumina filler and has a net thermal conductivity estimated to be  $1.5 \text{ W/m}\cdot\text{K}$ .

Attached to the top of this aluminum lid is a  $24.7 \times 27.9 \times 15.24 \text{ mm}$  aluminum extruded-fin heatsink with eight extruded fins, as seen in **Figure 3**. A  $50 \mu\text{m}$  thick layer of thermally conductive epoxy (thermal conductivity =  $\text{W/m}\cdot\text{K}$ ) is used to connect the lid and the heatsink base and denoted in the following as TIM2. **Table 1** displays the assembly dimensions and material conductivity.

## 2.2. Governing Equations and Boundary Conditions

The heat diffusion equation is the governing equation for the temperature of the items in the FC-PBGA/lid/ heatsink assembly. For steady state conditions, the heat diffusion equation for this assembly can be written as

$$\frac{\partial}{\partial x} \left( k_x \frac{\partial T}{\partial x} \right) + \frac{\partial}{\partial y} \left( k_y \frac{\partial T}{\partial y} \right) + \frac{\partial}{\partial z} \left( k_z \frac{\partial T}{\partial z} \right) + \dot{g} = 0 \quad (1)$$

where  $T$  is the temperature of the item,  $\dot{g}$  is the heat dissipation rate per unit volume in the chip and  $k_x$ ,  $k_y$ ,  $k_z$  are thermal conductivity in the  $x$ ,  $y$  and  $z$  directions.

The boundary conditions surrounding the assembly are heat convection and radiation to the ambient air. The heat

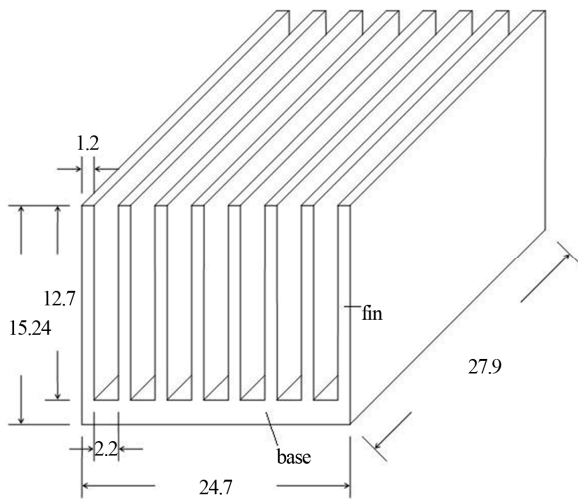


**Figure 3. Drawing of the extruded-fin heatsink.**

**Table 1. Assembly dimensions and material conductivities [8].**

Item	Dimension (mm)	Material	Conductivity (W/m·K)
Chip	$7.5 \times 5.4 \times 0.74$	Silicon	109.0
Solder Bump	0.127 diameter and 0.0762 height	90/10 Sn/Pb	36
Underfill		Epoxy with silica filler	0.6
Substrate	$25 \times 25 \times 1.0$	FR-5 core material, 4 metal layers, solder mask on top and bottom	0.35 for FR-5, 398 for Cu, 0.245 for mask
Solder ball	0.77 diameter and 0.45 height	40/60 Sn/Pb	50
PCB	$100 \times 100 \times 1.52$ , one top Cu trace layer (2oz) and two internal Cu planes (1oz), with thermal vias	FR-4 core material, 4 metal layers, solder mask on top and bottom	0.35 for FR-4, 398 for Cu, 0.245 for mask
Extruded-fin heatsink	$24.7 \times 27.9 \times 15.24$	Aluminum	226

loss to the ambient or outward heat flux through the exposed surface is

$$q = (h_c + h_r)(T_s - T_\infty) \quad (2)$$

in which  $T_s$  is the assembly surface temperature,  $T_\infty$  is the ambient air temperature,  $h_r$  is the radiation heat transfer coefficient and  $h_c$  is the convection heat transfer coefficient.

## 2.3. Finite Element Model

Under forced convection, the convection heat transfer coefficients  $h_c$  for the FC-PBGA/lid/heatsink assembly are calculated using the isothermal flat plate correlation equations previously applied by Mertol [9] as follows.

For the basic FC-PBGA assembly external surfaces,

$$h_c = 3.786\sqrt{V/L}, \quad (3)$$

where  $V$  is the airflow velocity in m/s and  $L$  is the total length in the flow direction in meters.

For the heatsink external surface,

$$h_c = 4.37\sqrt{V/L}, \quad (4)$$

where  $V$  again is airflow velocity in m/s and  $L$  is the average fin length in meters.

Under free convection, the convection heat transfer coefficient  $h_c$  for the FC-PBGA/lid/heatsink assembly is calculated as suggested by Ellison [10] for small devices encountered in the electronics industry as

$$h_c = f \left( \frac{\Delta T_{s-a}}{L_{ch}} \right)^n, \quad (5)$$

where  $\Delta T_{s-a}$  is the temperature difference in °C between the surface and the ambient air,  $f$  and  $n$  are empirical factors and  $L_{ch}$  is the package characteristic length in meters. The constants  $f$  and  $n$  are given as  $f = 0.83$  and  $n = 0.33$  for a horizontal plate facing upward,  $f = 0.415$  and  $n = 0.33$  for a horizontal plate facing downward, and  $f = 1.09$  and  $n = 0.35$  for a vertical plate. In the equation,  $L_{ch}$  is the characteristic length in meters. For horizontal plates,  $L_{ch} = W \cdot L / 2(W + L)$  where  $W$  and  $L$  are the respective width and length of a plate. For vertical plates,  $L_{ch} = H$ , where  $H$  is the vertical height of the plate.

When radiating, the radiation heat transfer coefficient  $h_r$  is calculated as

$$h_r = Bfe(T_s + T_\infty)(T_s^2 + T_\infty^2), \quad (6)$$

where  $B$  is the Boltzmann constant ( $B = 5.67 \times 10^{-8} \text{ W/m}^2/\text{K}^4$ ),  $e$  is the surface emissivity,  $f$  is the radiative view factor,  $T_s$  is the assembly surface temperature and  $T_\infty$  is the ambient air temperature.

The FC-PBGA/lid/heatsink assembly detailed above is represented by a three-dimensional finite element model using ANSYS finite element code. Due to the symmetric nature of both the heat problem and the assembly, only one quarter of the assembly is modeled. In the finite element analysis, an ambient temperature of 50°C, and a uniform chip power dissipation of 3 W is assumed. The model is complete enough to include key packaging elements such as bumps, solder balls, substrate, PCB, extruded-fin heatsink, lid, vias, TIM1, TIM2, lid-substrate adhesive, and ground planes for both signal and power.

## 2.4. Grid Refinement

Choice of node (or element) density in finite element solution procedures has a strong effect on the quality and computational cost. In this paper, variable grid spacing is used so that a finer spacing occurs in areas of relatively large gradients. Moreover, a grid dependency study is performed.

Three finite-element meshes (labeled M1, M2 and M3) with mesh densities of 168,850, 231,392 and 323,136 elements, respectively, are used to calculate the thermal resistance of the FC-PBGA/lid/heatsink assembly. The calculated results are shown in **Figure 4** for the cases of air speeds from 0 to 3 m/sec. Solutions using meshes M2 and M3 are virtually identical, indicating that M2 is sufficient to obtain reasonable solutions. Mesh M1 seems too coarse to produce adequate solutions. Since the intermediate density mesh M2 requires significantly less computational effort than the highest density M3, the M2

mesh shown in **Figure 5** is chosen as a good trade-off between accuracy and computational cost.

## 3. Results and Discussion

The ANSYS three-dimensional finite element analysis of the thermal characterization in the presented assemblies yielded the following results.

### 3.1. Temperature Analysis

The adding of an aluminum lid/heatsink significantly influences the thermal performance of the assembly. The temperature contours of the FC-PBGA assembly with/without an aluminum lid/heatsink for an airflow of zero are shown in **Figures 6** and **7**, respectively. In **Figure 6**, the maximum temperature occurs in the chip. With the addition of the lid/heatsink, as shown in **Figure 7**, the

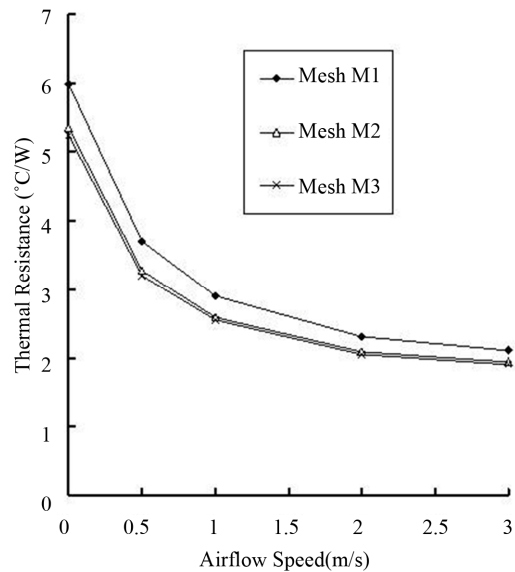


**Figure 4.** Relation between thermal resistance and airflow speed for FC-PBGA/lid/heatsink assembly using mesh M1, M2 and M3.

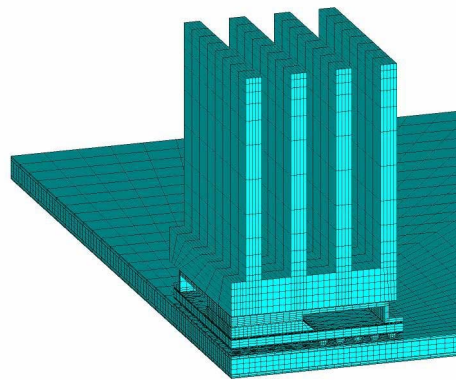


**Figure 5.** Finite element mesh M2 used in simulations for the FC-PBGA/lid/heatsink assembly.

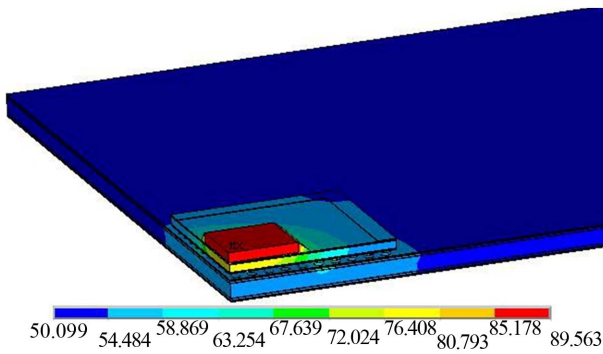


Figure 6. Temperature contours for the basic FC-PBGA assembly at airflow = zero.

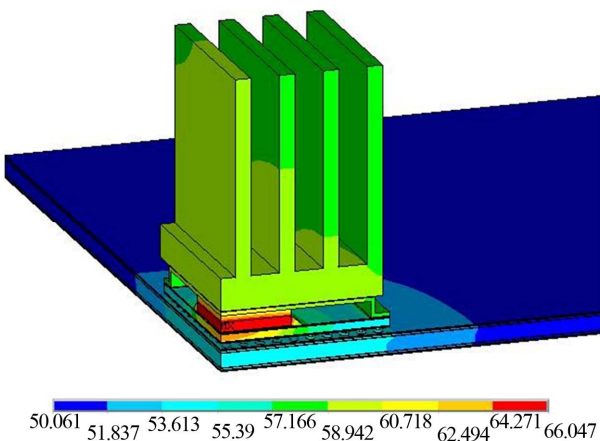


Figure 7. Temperature contours for the FC-PBGA/lid/heatsink assembly at airflow = zero.

maximum temperature still occurs in the chip. However, the maximum temperatures drop significantly. The temperature contours of the extruded-fin heatsink are shown in **Figure 8**, where the maximum temperature is found at the bottom center (remembering that the figure shows only one quarter of the extruded-fin heatsink since the total assembly is symmetrical), while the minimum temperature occurs at the outside corner of the most distant fin's upper edge. The temperature distribution in the extruded-fin heatsink is quite uniform due to the very high thermal conductivity of the aluminum material.

### 3.2. Thermal Resistance

As commonly done, thermal resistance ( $R_{ja}$ ) is used to characterize the thermal performance of an assembly, defined as

$$R_{ja} = \frac{(T_j - T_\infty)}{P} \quad (7)$$

where  $T_j$  is the predicted maximum temperature for the assembly,  $P$  the device power and  $T_\infty$  is the ambient air temperature.

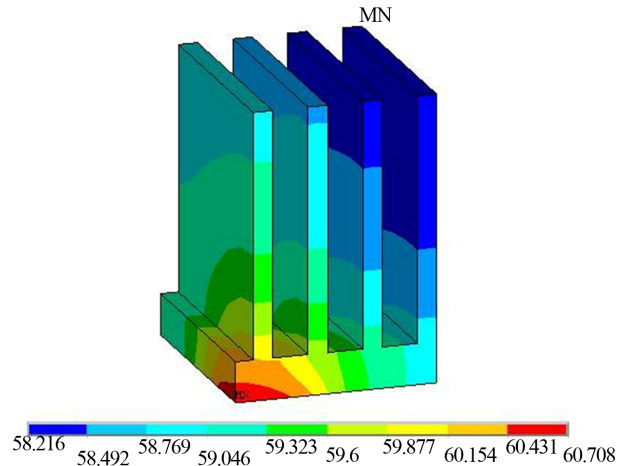


Figure 8. Temperature distribution for the extruded-fin heatsink at airflow = zero.

For comparison of thermal performance, four different FC-PBGA assembly versions are considered in this section and described as follows:

- 1) The basic FC-PBGA assembly (or the basic FC-PBGA model), defined as the FC-PBGA assembly without thermal enhancement shown in **Figure 1**;
- 2) Basic FC-PBGA model + lid, defined as the basic assembly with a lid attached on the top;
- 3) Basic FC-PBGA model + heatsink, defined as the basic assembly with an extruded-fin heatsink attached on the top;
- 4) Basic FC-PBGA model + lid/heatsink, defined as the basic assembly with a lid attached on top, after which an extruded-fin heatsink is attached on the top of the lid (*i.e.* FC-PBGA/lid/heatsink shown in **Figure 2**).

**Figure 9** shows the thermal performance of the above four cases for airflows ranging from 0 to 3 m/sec. Addition of the lid to the basic FC-PBGA model (*i.e.* basic FC-PBGA model + lid) causes significant improvement in thermal performance. The high thermal conductivity of the aluminum lid results in a larger surface area with a temperature high enough for good convective cooling. Addition of only the extruded-fin heatsink to the basic model (*i.e.* basic FC-PBGA model + heatsink) causes large improvement in thermal performance relative to the basic FC-PBGA model due to the large increase in heat transfer area. Addition of the lid between the basic FC-PBGA model and the extruded-fin heatsink (*i.e.* basic FC-PBGA model + lid/heatsink or FC-PBGA/lid/heatsink) results in a small further improvement in thermal performance. This small further increase can be attributed to the increased cooling area made available by the sides of the lid. Clearly, the increased cooling area presented by the sides of the lid is small relative to the large total cooling area of the extruded-fin heatsink. The role of the lid is interesting. If an extruded-fin heatsink is not applied to the basic model, then addition of the lid results in significant

improvement of thermal performance. On the other hand, if a extruded-fin heatsink has been applied to the basic FC-PBGA model, then the further addition of the lid does not result in significant further improvement of thermal performance.

Inspection of **Figure 9** shows that, at an airflow of zero, the predicted  $R_{ja}$  of the FC-PBGA/lid/heatsink is about 57.0% lower than the basic PBGA assembly. If progressively faster air flow is applied to the FC-PBGA/lid/heatsink, then the improvement of the FC-PBGA/lid/heatsink relative to the basic FC-PBGA assembly at air-flow = zero increases with increasing air speed, reaching a maximum improvement of 84.9% at this study's maximum airspeed of 3 m/s.

### 3.3. Effects of Design Parameters

Thermal performance is analyzed by considering various design parameters of the polymer-based materials and the thermal enhancement components. The polymer-based materials include underfill, TIM1, TIM2, lid-substrate adhesive and substrate core material. The specific thermal enhancement components are the lid and the extruded-fin heatsink. Effects of the design parameters are studied by varying the parameter values by 30% for all material conductivities and by 15% for all material dimensions in both natural ( $v = 0$ ) and forced convection ( $v = 1$ ) environments. Simulation results are shown in **Figures 10-13**.

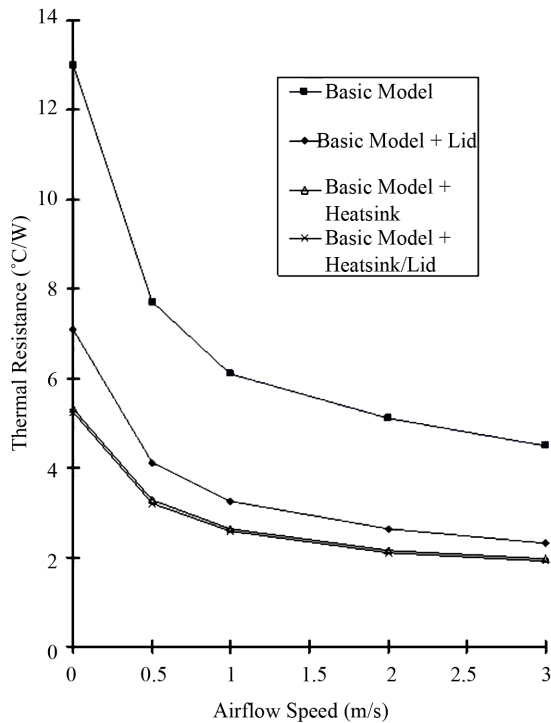


**Figure 9.** Relation between thermal resistance and airflow speed for four different assembly configurations.

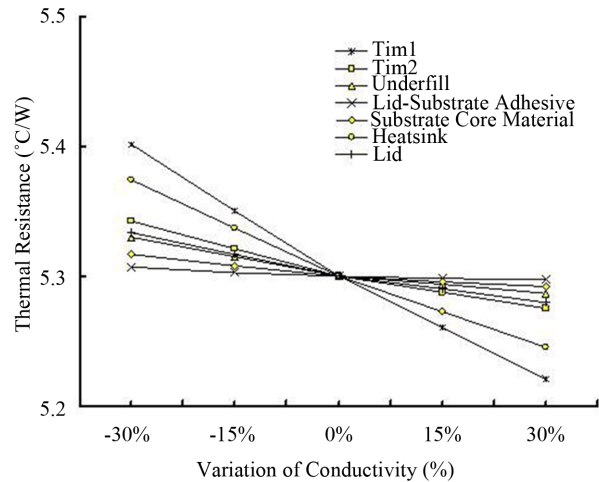


**Figure 10.** Relation between thermal resistance and thermal conductivity in natural convection condition ( $v = 0$ ).

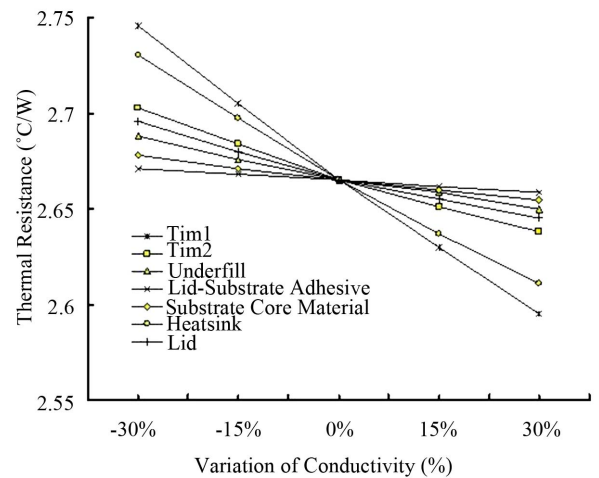


**Figure 11.** Relation between thermal resistance and thermal conductivity in forced convection condition ( $v = 1$ ).

#### 3.3.1. Effect of Extruded-Fin Heatsink

Extruded-fin heatsink design has significant effect on thermal performance of the assembly. The effects of extruded-fin heatsink conductivity with regard to thermal performance of the assembly can be found in **Figures 10** and **11** for both natural and forced convection environments, respectively. Increased extruded-fin heatsink conductivity increases the thermal performance of the assembly since higher thermal conductivity improves the heat spreading effect in the heatsink. **Figure 14** further shows the thermal resistance  $R_{ja}$  vs the thermal conductivity of the extruded-fin heatsink for airflows ranging from 0 to 3 m/sec. The results show little improvement in performance at thermal conductivities above 200 W/m·K. Thus, little advantage can be obtained by using copper (thermal conductivity = 393 W/m·K) relative to aluminum (thermal conductivity = 226 W/m·K).

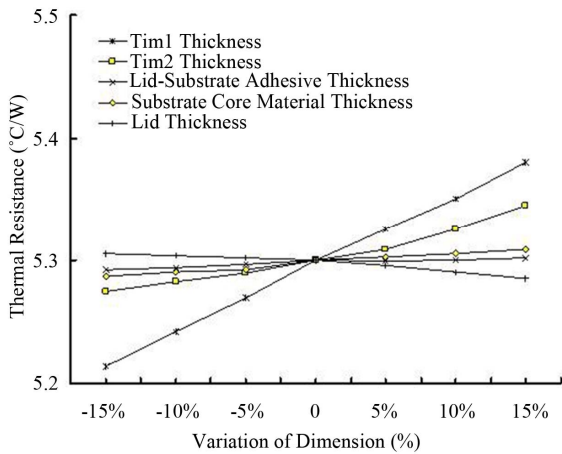


Figure 12. Relation between thermal resistance and dimensions in natural convection condition ( $\nu = 0$ ).

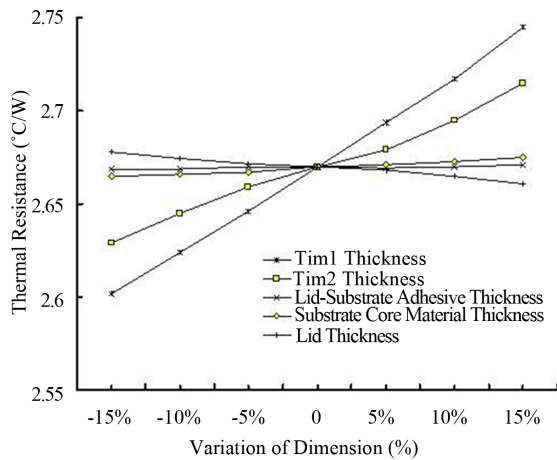


Figure 13. Relation between thermal resistance and dimensions in forced convection condition ( $\nu = 1$ ).

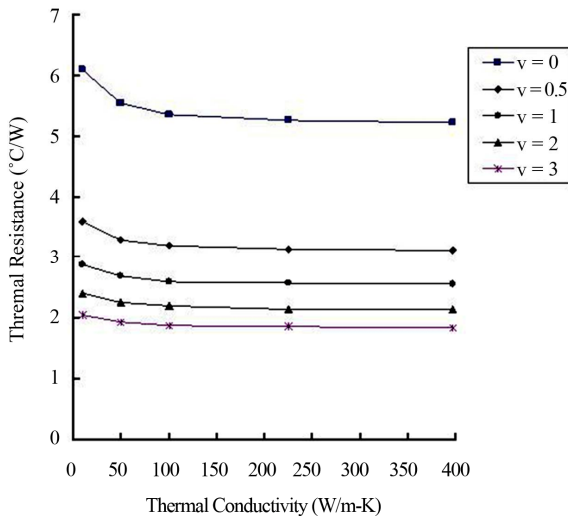


Figure 14. Relation between thermal resistance and extruded-fin heatsink conductivity.

This observation is of interest to designers with regard to material selection.

Effects of fin length, fin thickness, fin number and base thickness of the extruded-fin heatsink on thermal resistance  $R_{ja}$  are presented for the FC-PBGA/lid/heatsink assembly. Increasing the number of fins or the length of the fins decreases the thermal resistance  $R_{ja}$  due to the increase of heatsink cooling area, as shown in Figures 15 and 16, for both natural ( $\nu = 0$ ) and forced convection ( $\nu = 1$ ) environments.

It is seen that  $R_{ja}$  improves as the base thickness increases because increased base thickness increases the total cooling area of the heatsink and improves the cooling efficiency of the heatsink. But the improvement is small and the resulting material cost could be higher.

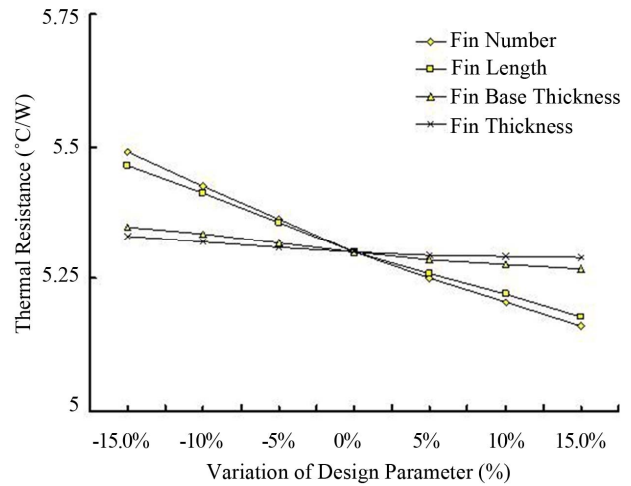


Figure 15. Relation between thermal resistance and design parameters of extruded-fin heatsink in natural convection condition ( $\nu = 0$ ).

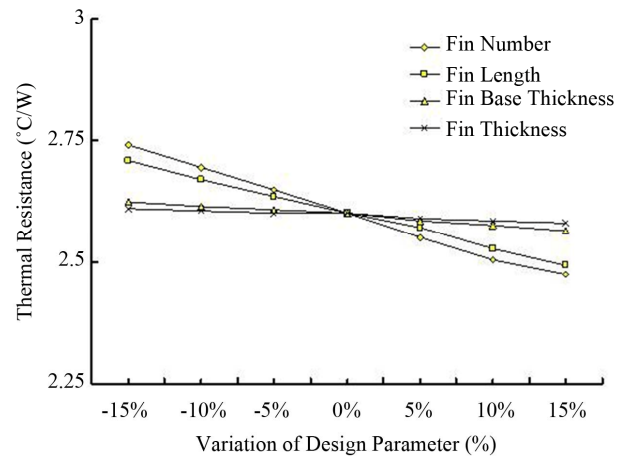


Figure 16. Relation between thermal resistance and design parameters of extruded-fin heatsink in forced convection condition ( $\nu = 1$ ).

Increasing the fin thickness increases the total cooling area of the heatsink. However this increased cooling area is very small compared with the total area of the heatsink, so the results show only a slight effect for fin thickness and can be neglected.

### 3.3.2. Effect of the Lid

The purpose of lid is to protect the chip and improve heat spreading from the chip. Effect of thermal conductivity of the lid on the thermal performance of the assembly for both natural and forced convection environments can also be found in **Figures 10** and **11**, respectively. Increased lid conductivity increases the thermal performance of the assembly.

Specific variance of the thermal resistance  $R_{ja}$  relative to the lid thickness is shown in **Figures 12** and **13** for both natural and forced convection environments. The results shows a small improvement in  $R_{ja}$  as thickness increases.

### 3.3.3. Effect of Underfill

The purpose of the underfill is to release the thermo-mechanical stress of the solder bumps due to CTE mismatch between the silicon chip and the organic substrate. Increased thermal conductivity of the underfill increases the heat conduction in the package and is helpful for dissipating heat to the ambient atmosphere. Thus, increasing the conductivity of the underfill increases the thermal performance of the assembly.

### 3.3.4. Effect of TIM1 and TIM2

The effects of TIM1 and TIM2 on the thermal performance of the assembly for both natural and forced convection environments can also be found in **Figures 10-13**.

As TIM1's or TIM2's conductivity increases, the thermal performance of the assembly increases, since increased conductivity of TIM1 or TIM2 reduces the thermal resistance in the heat transfer path. Also, it can be found in **Figures 12** and **13** that as TIM1's or TIM2's thickness decreases, the thermal performance of the assembly increases, since decreased thickness of TIM1 or TIM2 reduces the thermal resistance in the heat transfer path. Simulation results show that TIM1 has a greater influence on assembly thermal performance than TIM2.

### 3.3.5. Effect of Substrate Core Material

The effect of the thermal conductivity of the substrate core material on the thermal performance of the assembly can also be found in **Figures 10** and **11**. Increasing the conductivity of the substrate core material increases heat transfer from chip to ambient, but the amount of heat conducted through this pathway is quite small relative to the amount conducted through the vias and heatsink. Thus, thermal performance increases with increas-

ing conductivity of the substrate core material, but the effect is small.

Thicker substrate core material reduces the thermal performance of the assembly due to a longer thermal path for heat transfer to the PCB. Thus thermal performance decreases with increasing thickness of the substrate core material but the effect is small, as seen in **Figures 12** and **13**.

### 3.3.6. Effect of Lid-Substrate Adhesive

An adhesive material is required to form a good bond between the lid and the substrate. The effects of the conductivity and thickness of the adhesive with regard to the thermal performance of the assembly are also shown in **Figures 10-13**. It is found that these effects are all relatively insignificant, but higher conductivity and smaller thickness are preferred.

## 4. Conclusions

Three-dimensional finite element simulation has been used to study the thermal performance of a thermally enhanced FC-PBGA assembly in both natural and forced air convection environments. The thermally enhanced FC-PBGA assembly is a basic FC-PBGA assembly with a lid attached on top, after which an extruded-fin heatsink is attached on the top of the lid. The adding of an aluminum lid/heatsink significantly influences the thermal performance of the assembly due to the large increase in heat transfer area. Also, the temperature distribution in the extruded-fin heatsink is quite uniform due to the very high thermal conductivity of the aluminum material. If a extruded-fin heatsink is not applied to the basic model, then addition of the lid results in significant improvement of the thermal performance. On the other hand, if an extruded-fin heatsink has been applied to the basic model, then further addition of the lid does not result in significant further improvement of thermal performance, because the increased cooling area presented by the sides of lid is little relative to the large total cooling area of the heatsink.

A series of parametric simulations investigate the effects of varying the design parameters of the polymer-based materials and the thermal enhancement components. Conclusions from the analysis are summarized as follows:

- 1) Extruded-fin heatsink design has significant effects on the thermal performance of the assembly. Higher thermal conductivity improves the thermal performance of the assembly. However, results show little improvement in performance at thermal conductivities above 200 W/m·K. Thus, little advantage can be obtained by using copper (thermal conductivity = 393 W/m·K) relative to aluminum (thermal conductivity = 226 W/m·K). This observation is of interest to designers with regard to ma-

terial selection. Increasing the fin length, fin number, and base thickness of the extruded-fin heatsink results in increased thermal performance of the assembly. For the cases studied, simulation results show that the fin length and fin number have a stronger influence on the thermal performance than base thickness. The effect of fin thickness is negligibly small.

2) As for conductivity, when TIM1 or TIM2 increases or the thickness of TIM1 or TIM2 decreases, the thermal performance of the assembly increases. Simulation results show that TIM1 has a stronger influence on assembly thermal performance than TIM2.

3) As conductivity of the underfill increases, thermal performance of the assembly increases but the improvement is not very significant.

4) It is found that as the thickness of the substrate core decreases, thermal performance of the assembly increases. Thermal performance of the assembly can be enhanced by using a thinner core. Also, higher conductivity of the substrate core is desirable for better thermal performance of the assembly.

5) The effects of the lid-substrate adhesive parameters are also considered and found to have lesser impact on package thermal performance. However, higher conductivity and lower thickness of the lid-substrate adhesive are found preferable.

## REFERENCES

- [1] G. H. Wu, S.H. Ju and T. C. Tsein, "Three-Dimensional Finite Element Analysis of Thermomechanical Behavior in Flip-Chip Packages under Temperature Cycling Conditions," *Journal of Reinforced Plastics and Composites*, Vol. 24, No. 18, 2005, pp. 1895-1907. [doi:10.1177/0731684405054333](https://doi.org/10.1177/0731684405054333)
- [2] F. Gugliemmermetti and S. Grignaffini, "Direct Approach to the Design of Plate Fin Heat Sinks Stack Cooled by Forced Convection," *IEEE Electronic Packaging Technology Conference*, San Diego, 8-10 December 1998, pp. 138-142.
- [3] B. Joiner, "Thermal performance of Flip Chip Ball Grid Arrays Packages," *Eighteenth Annual IEEE Semiconductor Thermal Measurement and Management Symposium*, San Jose, 12-14 March 2002, pp. 50-56.
- [4] K. M. Chen, K. H. Houg and K. N. Chiang, "Thermal Resistance Analysis and Validation of Flip Chip PBGA Packages," *Microelectronics Reliability*, Vol. 46, No. 2-4, 2006, pp. 440-448. [doi:10.1016/j.microrel.2005.06.001](https://doi.org/10.1016/j.microrel.2005.06.001)
- [5] Z. Luo, H. Cho and K. Cho, "System Thermal Analysis of Mobile Phone," *Applied Thermal Engineering*, Vol. 28, No. 14-15, 2008, pp. 1889-1895. [doi:10.1016/j.applthermaleng.2007.11.025](https://doi.org/10.1016/j.applthermaleng.2007.11.025)
- [6] A. R. Menon, S. Karajgikar and D. Agonafer, "Thermal Design Optimization of a Package on Package," *25th Annual IEEE Semiconductor Thermal Measurement and Management Symposium (Semi-Therm)*, San Jose, 15-19 March 2009, pp. 329-336.
- [7] "ANSYS User's Manual, Revision 13.0," Swanson Analysis System Inc., Houston, 2010.
- [8] T.-Y. Lee, "An Investigation of Thermal Enhancement on Flip Chip Plastic BGA Packages Using CFD Tool," *IEEE Transactions on Components, Packaging, and Manufacturing Technology*, Vol. 23, No. 3, 2000, pp. 481-489. [doi:10.1109/6144.868847](https://doi.org/10.1109/6144.868847)
- [9] A. Mertol, "Thermal Performance Comparison of High Pin Count Cavity-Up Enhanced Plastic Ball Grid Array (EPBGA) Packages," *IEEE Transactions on Components, Packaging, and Manufacturing Technology, Part B*, Vol. 19, No. 2, 1996, pp. 427-443.
- [10] G. N. Ellison, "Thermal Computations for Electronic Equipment," E. Robert Krieger Publishing Company, Malabar, 1989.

## Nomenclature

$f$  : empirical factor.  
 FC-PBGA: flip-chip plastic ball grid array.  
 $\dot{q}$  : heat dissipation rate per unit volume in the chip,  $W/m^3$ .  
 $k$  : thermal conductivity,  $W/m \cdot K$ .  
 $k_x$  : thermal conductivity in the  $x$  direction,  $W/m \cdot K$ .  
 $k_y$  : thermal conductivity in the  $y$  direction,  $W/m \cdot K$ .  
 $k_z$  : thermal conductivity in the  $z$  direction,  $W/m \cdot K$ .  
 $h_c$  : convection heat transfer coefficient,  $W/m^2 \cdot K$ .  
 $h_{rad}$  : radiation heat transfer coefficient,  $W/m^2 \cdot K$ .  
 $L_{ch}$  : characteristic length, m.

$n$  : empirical factor.  
 $P$  : device power,  $W$ .  
 PCB: printed circuit board.  
 $\Delta T_{s-a}$  : temperature difference between the surface and the ambient air,  $^{\circ}C$ .  
 $T_{\infty}$  : ambient air temperature,  $^{\circ}C$ .  
 $R_{ja}$  : thermal resistance of the assembly,  $^{\circ}C/W$ .  
 $T$  : temperature,  $^{\circ}C$ .  
 $T_j$  : predicted maximum temperature of an assembly,  $^{\circ}C$ .  
 $T_s$  : surface temperature of the assembly,  $^{\circ}C$ .  
 $V$  : air velocity, m/s.